



### Explaining the Unusual Photoluminescence of Semiconductor Nanocrystals Doped Via Cation Exchange

Abigail Freyer, Peter Sercel, Zhentao Hou, Benjamin H. Savitzky,  
Lena F. Kourkoutis, Alexander Lev Efros, and Todd D. Krauss

*Nano Lett.*, Just Accepted Manuscript • DOI: 10.1021/acs.nanolett.9b02284 • Publication Date (Web): 14 Jun 2019

Downloaded from <http://pubs.acs.org> on June 20, 2019

#### Just Accepted

"Just Accepted" manuscripts have been peer-reviewed and accepted for publication. They are posted online prior to technical editing, formatting for publication and author proofing. The American Chemical Society provides "Just Accepted" as a service to the research community to expedite the dissemination of scientific material as soon as possible after acceptance. "Just Accepted" manuscripts appear in full in PDF format accompanied by an HTML abstract. "Just Accepted" manuscripts have been fully peer reviewed, but should not be considered the official version of record. They are citable by the Digital Object Identifier (DOI®). "Just Accepted" is an optional service offered to authors. Therefore, the "Just Accepted" Web site may not include all articles that will be published in the journal. After a manuscript is technically edited and formatted, it will be removed from the "Just Accepted" Web site and published as an ASAP article. Note that technical editing may introduce minor changes to the manuscript text and/or graphics which could affect content, and all legal disclaimers and ethical guidelines that apply to the journal pertain. ACS cannot be held responsible for errors or consequences arising from the use of information contained in these "Just Accepted" manuscripts.

1  
2  
3 **Explaining the Unusual Photoluminescence of Semiconductor Nanocrystals Doped Via**  
4 **Cation Exchange**  
5  
6  
7  
8  
9

10 *Abigail R. Freyer<sup>†</sup>, Peter C. Sercel<sup>§</sup>, Zhentao Hou<sup>†</sup>, Benjamin H. Savitzky<sup>‡, #</sup>, Lena F.*  
11 *Kourkoutis<sup>–||</sup>, Alexander L. Efros<sup>¶</sup>, Todd D. Krauss<sup>\*, †, £</sup>*  
12  
13  
14  
15  
16

17 <sup>†</sup>Department of Chemistry and <sup>£</sup>The Institute of Optics, University of Rochester, Rochester, New  
18 York 14627-0216, United States  
19  
20  
21  
22  
23

24 <sup>§</sup>T. J. Watson Laboratory of Applied Physics, California Institute of Technology, Pasadena,  
25 California 91125, United States  
26  
27  
28  
29  
30

31 <sup>‡</sup>Department of Physics, <sup>–</sup>School of Applied and Engineering Physics, <sup>||</sup>Kavli Institute at Cornell  
32 for Nanoscale Science, Cornell University, Ithaca, New York 14853, United States  
33  
34  
35  
36  
37

38 <sup>¶</sup>Naval Research Laboratory, Washington, D.C. 20375, United States  
39  
40  
41  
42

43 <sup>\*</sup>Corresponding author. E-mail: krauss@chem.rochester.edu  
44  
45  
46  
47  
48  
49  
50  
51  
52  
53  
54  
55  
56  
57  
58  
59  
60

#Current address: Department of Chemistry, Brown University, Providence, Rhode Island 02912,  
United States

### Abstract

Aliovalent doping of CdSe nanocrystals (NCs) via cation exchange processes has resulted in interesting and novel observations for the optical and electronic properties of the NCs. However, despite over a decade of study, these observations have largely gone unexplained, partially due to an inability to precisely characterize the physical properties of the doped NCs. Here, electrostatic force microscopy was used to determine the static charge on individual, cation-doped CdSe NCs in order to investigate their net charge as a function of added cations. While the NC charge was relatively insensitive to the relative amount of doped cation per NC, there was a remarkable and unexpected correlation between the average NC charge and PL intensity, for all dopant cations introduced. We conclude that the changes in PL intensity, as tracked also by changes in NC charge, are likely a consequence of changes in the NC radiative rate caused by symmetry breaking of the electronic states of the nominally spherical NC due to the Coulombic potential introduced by ionized cations.

**Keywords:** semiconductor nanocrystals, aliovalent doping, cation exchange, electrostatic force microscopy, nanocrystal charge, symmetry breaking

1  
2  
3  
4  
**Paper**5  
6  
7  
8  
9  
10  
11  
12  
13  
14  
15  
16  
17  
18  
19  
20  
21  
22  
23  
24  
25  
26  
27  
28  
29  
30  
31  
32  
33  
34  
35  
36  
37  
38  
39  
40  
41  
42  
43  
44  
45  
46  
47  
48  
49  
50  
51  
52  
53  
54  
55  
56  
57  
58  
59  
60  
For decades, semiconductor nanocrystals (NCs) have been studied for their interesting electrical and optical properties,<sup>1,2,3</sup> which also make them potentially suitable for a number of applications, including solar energy conversion<sup>4,5,6</sup>, optoelectronic devices<sup>7,8,9,10</sup>, and biomedical imaging<sup>11,12,13,14</sup>. Major advances in the colloidal NC field directly arose from the ability to control the composition, size, and morphology of NCs, which is made possible by a number of different synthesis techniques.<sup>15,16</sup> Cation exchange, a chemical transformation used to modify a crystal whereby a cation from solution is inserted or exchanged with a host cation, has recently become a highly effective tool for enabling the synthesis of nanoparticles with novel chemical compositions.<sup>17,18</sup> Cation exchange has been used to synthesize novel core/shell NCs<sup>19</sup>, branched NC structures<sup>20</sup>, heterostructured nanorods<sup>21,22</sup>, and core and core/shell nanoplatelets<sup>23</sup>, NC compositions and morphologies that are otherwise unobtainable by direct synthesis.31  
32  
33  
34  
35  
36  
37  
38  
39  
40  
41  
42  
43  
44  
45  
46  
47  
48  
49  
50  
51  
52  
53  
54  
55  
56  
57  
58  
59  
60  
Cation exchange has also been used to dope NCs by carefully controlling the number of cations in solution that become available for exchange.<sup>24,25</sup> Doping of NCs can also be achieved through a variety of other methods, including nucleation and growth doping<sup>26</sup>, surface treatments<sup>27,28</sup>, and etching-regrowth-doping<sup>29</sup>, but cation exchange has become one of the more popular techniques due to its relative simplicity.<sup>30</sup> Doping NCs via cation exchange is advantageous since it affords supposedly excellent control over doping levels while also allowing for undoped control samples for facile evaluation of the effects of doping on the NC.<sup>24</sup> While a number of synthesis methods and doped NC systems are available and have been studied<sup>24,25,30,31,32,33,34,35,36</sup>, many effects of doping on the photophysics of NCs are not well understood. Specifically, we focused on the cation exchange aliovalent doping of CdSe NCs with Ag<sup>+</sup> to produce series of samples that differ only by the amount of Ag added.<sup>25</sup> These Ag<sup>+</sup>

1  
2  
3 doped CdSe NCs demonstrate unusual photophysics whereby a substantial increase in the  
4 exciton photoluminescence (PL) intensity was observed upon doping with a small amount of Ag<sup>+</sup>  
5 followed by a subsequent decrease in PL intensity with further increasing doping amounts.<sup>25</sup>  
6  
7 Additionally, a dopant “defect” PL peak also grew in to the red of the main band-edge peak with  
8 increasing dopant amount. Recently, it was found that introducing Ag<sup>+</sup> during a one-pot  
9 synthesis/cation exchange procedure resulted in a broad, intense dopant PL peak with no exciton  
10 PL.<sup>37</sup> These divergent behaviors exemplify the need for greater understanding about the cation  
11 exchange doping process of NCs in general, and in particular, about how Ag<sup>+</sup> dopants affect NC  
12 PL.  
13  
14

15 Doping of NCs via cation exchange could result in the creation of locally charged  
16 particles depending on the nature of the doping process.<sup>29</sup> For example, the introduction of the  
17 aliovalent Ag<sup>+</sup> impurity ion as an interstitial dopant would cause a locally positive charge inside  
18 the NC. Conversely, the introduction of Ag<sup>+</sup> as a substitutional dopant would result in a locally  
19 negative charge as the Cd<sup>2+</sup> ions are displaced from the crystal lattice. We hypothesized that  
20 direct measurements of the charged state of the doped NCs as a function of the added Ag<sup>+</sup> per  
21 NC could provide insight into the unusual exciton photoluminescence properties reported for Ag<sup>+</sup>  
22 doped CdSe NCs,<sup>25</sup> as well as provide a greater understanding of the cation exchange doping  
23 process itself.  
24  
25

26 Here we report a dramatic and unexpected relationship between the charges of individual  
27 CdSe NCs doped with Ag<sup>+</sup> and the photoluminescence properties for these NC samples.  
28 Specifically, we found that as the number of dopant ions per NC was varied, the subsequent  
29 changes in the ensemble exciton PL intensity and the average electrostatic charge per NC as  
30 determined with electrostatic force microscopy (EFM) were highly correlated. Conversely, the  
31  
32  
33  
34  
35  
36  
37  
38  
39  
40  
41  
42  
43  
44  
45  
46  
47  
48  
49  
50  
51  
52  
53  
54  
55  
56  
57  
58  
59  
60

average charge measured per NC did not seem to depend strongly on the quantity of dopant ions added during the cation exchange process. Indeed, despite adding between one and hundreds of  $\text{Ag}^+$  dopant ions on average per CdSe NC, the average charge measured using EFM never varied by more than  $\pm 1\text{e}$ . We further show this fixed and stable charge results from both the cation exchange process (i.e. replacing a +2 cation with a +1 cation and/or a +1 cation interstitial), and the attraction of counterions to the charged NC surface. By calculating the radiative rate for CdSe NCs of various configurations of charges near the surface of the NC, we accurately modeled both the changes in the charge state of the NC and the changes in PL intensity, thus showing that the combination of surface and interior charges due to doping can explain the observed photophysical behavior.

CdSe NCs were made using variations on known synthesis procedures<sup>38,39</sup> and were then doped with  $\text{Ag}^+$ ,  $\text{Li}^+$ , or  $\text{Ca}^{2+}$  ions using a cation exchange procedure adapted from Sahu *et al.*<sup>25</sup> The amount of dopant introduced into the NC was quantified using inductively coupled plasma mass spectrometry (ICP-MS). Absorption spectroscopy showed little to no change in the absorbance with increasing dopant concentration, even at extremely high doping amounts, as seen in Figure 1a. Enhancement in the exciton PL intensity with increasing added  $\text{Ag}^+$  was sometimes observed (though not always) while a dopant peak consistently grew in to the red of the main peak with increasing  $\text{Ag}^+$  added, as evident in Figure 1b. These trends in PL spectra also agree with the trends reported for  $\text{Ag}^+$  doped CdSe NCs in Reference 25. From dark-field, high-resolution scanning transmission electron microscopy (ADF-STEM) (Figure 1c), one can see that the size, shape, and crystal structure of the NCs also remain unchanged with added dopants, as expected for doping via cation exchange processes.

Similar optical spectra were measured for doping controls in which the CdSe NCs were doped with  $\text{LiNO}_3$ ,  $\text{Ca}(\text{NO}_3)_2$ , and  $\text{AgClO}_4$  (Supporting Information Figures S12 and S13). Importantly, similar trends in absorbance and PL spectra were observed for these control samples. Thus, the exciton PL changes observed for  $\text{AgNO}_3$  doping are not due exclusively to the  $\text{Ag}^+$  cations acting as internal dopants within the NCs. Rather, the changes in exciton PL are due to the mere presence of a charged cation in the interior or on the surface of the NC. Note that while we observed changes in the exciton PL peak intensity with all dopants, the red-shifted dopant PL peak was only present with introduction of the  $\text{Ag}^+$ , both with  $\text{AgNO}_3$  and  $\text{AgClO}_4$  added, but not the  $\text{Li}^+$  or  $\text{Ca}^{2+}$  cations. This is expected behavior as this peak is attributed to the presence of the  $\text{Ag}^+$  as a dopant within the CdSe lattice.<sup>25,37</sup>

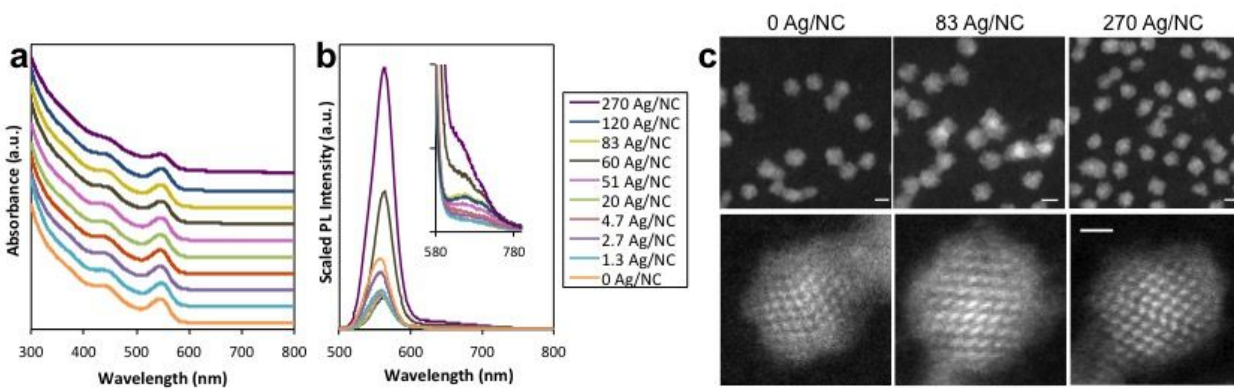


Figure 1. (a) Absorbance and (b) PL spectra for a series of  $\text{Ag}^+$  doped CdSe NCs. The inset in (b) magnifies the weak PL feature near 700 nm. (c) ADF-STEM images for three samples with different doping levels, (left) 0 Ag/NC, (middle) 83 Ag/NC, (right) 270 Ag/NC. Scale bars in the top images represent 3 nm and scale bar in the bottom image represents 1 nm.

EFM is an exceptionally sensitive technique that can be used to measure the charged state of single NCs to less than 1 elementary charge  $e$ .<sup>40,41,42,43,44</sup> EFM is a modification of atomic force microscopy that works by measuring the long-range electrostatic forces between a conductive cantilever and a conductive substrate. In our EFM experiment, a first pass of the

1  
2  
3 cantilever measures the topography of the sample. In a subsequent second pass, the tip is lifted  
4 off the surface and scanned at a constant height under an applied AC and DC voltage, and  
5 thereby is sensitive to long-range capacitive and Coulombic forces (See SI for a detailed  
6 description of EFM).<sup>41,43</sup>  
7  
8

9 Representative samples of EFM images are shown in Figure 2 for two different Ag<sup>+</sup>  
10 doped CdSe NC samples with 0 Ag/NC (top) and 0.5 Ag/NC (bottom). Images 2a and 2e are  
11 standard AFM height images and are used to identify the location and heights of the individual  
12 NCs. Images 2b and 2f correspond to the changes in cantilever resonance frequency at the first  
13 harmonic of the AC voltage  $\Delta\nu(\omega)$ , from which the charges of the individual NCs located in the  
14 height image are calculated (See SI for details of calculation). Images 2c and 2g correspond to  
15 changes in the cantilever resonance frequency at the second harmonic of the AC voltage  $\Delta\nu(2\omega)$   
16 and give information that depends on the dielectric constant of the individual NCs. Our  
17 measured dielectric constants for individual NCs were consistent with previously reported values  
18 for CdSe<sup>41,45,46</sup>, suggesting accurate modeling of the tip-substrate capacitance. Each NC sample  
19 exhibited a distribution of calculated charges. As shown in Figure 2f, the NCs doped with about  
20 0.5 Ag/NC are predominantly bright, indicating negatively charged NCs. Conversely, the NCs  
21 with 0 Ag/NC shown in Figure 2b are less bright, representing more neutral NCs. The NCs also  
22 contain a distribution in measured charge per NC as shown in the histograms, Figures 2d and 2h.  
23 EFM images for this entire doping series are shown in Fig. S7.  
24  
25  
26  
27  
28  
29  
30  
31  
32  
33  
34  
35  
36  
37  
38  
39  
40  
41  
42  
43  
44  
45  
46  
47  
48  
49  
50  
51  
52  
53  
54  
55  
56  
57  
58  
59  
60

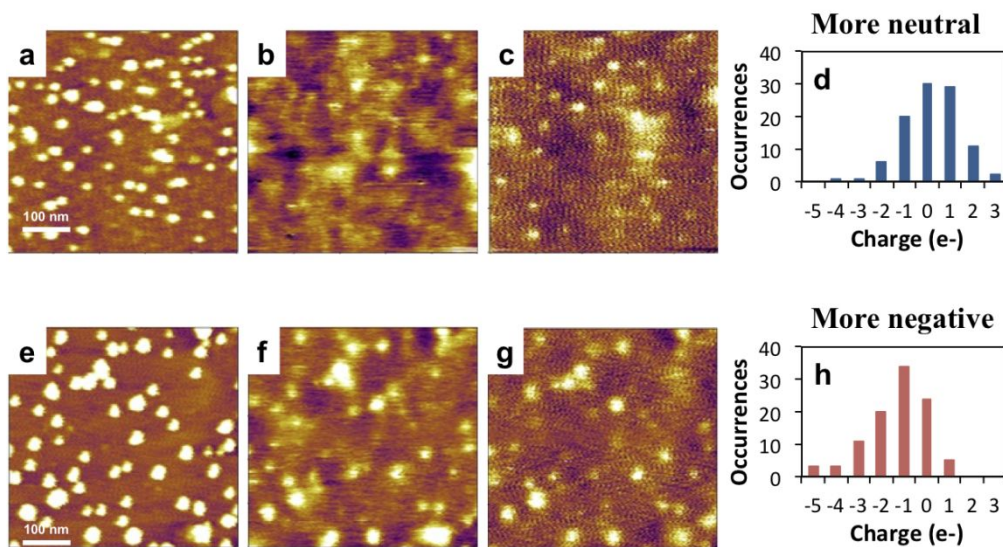


Figure 2. EFM images for samples with 0 Ag/NC (top) and 0.5 Ag/NC (bottom). (a,e) AFM height images, (b,f) charge images measuring cantilever response at  $\Delta v(\omega)$ , (c,g) dielectric constant images measuring cantilever response at  $\Delta v(2\omega)$ . (d,h) Histograms showing the distributions of NC charges in the corresponding EFM images.

For a given dopant quantity of Ag/NC, we used the mean value of the charge distribution to determine the average charge per NC. We then used these average values to plot the average charge per NC as a function of doping amount, as presented in Figure 3a. Similar data were acquired for the doping control samples  $\text{AgClO}_4$ ,  $\text{LiNO}_3$ , and  $\text{Ca}(\text{NO}_3)_2$  and are shown in Figure 3c. While CdSe NCs as synthesized are nominally neutral<sup>41</sup>, after the washing and rinsing process with no cation exchange (i.e. the undoped sample), the average charge per NC as measured with EFM ranged from -0.5 to -2.0 e. We presume that this negative charge results from a slight loss of metal carboxylate passivating ligands from the NC surface during the exposure to ethanol, leaving unpassivated Se anions.<sup>47</sup> Note that with respect to the average charge per NC, we could not find a simple monotonic trend with increasing dopant added, nor did we find consistent relationships between charge and dopant level among several doping trials. Corresponding plots of the maximum PL intensities vs. dopant concentration for these same sets of samples are also given in Figure 3 (b, d). Over several trials, we generally (but not

1  
2  
3 always) observed an initial increase in exciton PL intensity with added dopant, consistent with  
4 previous reports on Ag<sup>+</sup> doping of CdSe NCs Sahu *et al.*<sup>25</sup> Note that we did not observe an  
5 enhanced PL intensity due to Ag doping for every trial and there was no consistent trend in  
6 exciton PL intensity with respect to average Ag/NC amounts (see Supporting Information  
7 Figures S8-S11). Additionally, some trials show an overall decrease in the PL intensity,  
8 attributed to the substantial washing and workup procedures used for the doping process.  
9  
10 Further, the inability to reproducibly create homogenously doped NCs with this post-synthesis  
11 cation exchange process makes it impossible to obtain identical results across all doping trials.  
12  
13 We believe that the inconsistency and non-monotonic nature of the PL intensity enhancement  
14 with added Ag is due to the absence of an asymmetrical charge placement around the NC, as  
15 discussed subsequently.  
16  
17

18 In comparing the EFM and the PL data for the Ag<sup>+</sup> doped CdSe samples (Figures 3a and  
19 b) we found a remarkable correlation between the average charge per NC and the exciton PL  
20 intensity. Increases or decreases in NC charge tracked similar increases or decreases in the PL  
21 intensity, as the amount of Ag<sup>+</sup> was varied. It is important to note that the EFM and PL  
22 experiments are completely unrelated except for the sample: the former is an average over  
23 hundreds of NCs that are dried on a graphene substrate and the latter is an ensemble  
24 measurement in solution. This result suggests that the PL intensity changes seen across dopant  
25 levels are intimately associated with a charging event due to the introduction of anions and  
26 cations to the NCs. Considering the significant evidence that the Ag<sup>+</sup> impurity ions are  
27 introduced interstitially with eventual conversion to substitutional dopants<sup>25,48,49</sup> and the lack of a  
28 trend in the charge with respect to the dopant amount, the PL intensity changes are likely not  
29 exclusively due to the internal dopants. Further evidence for this hypothesis comes from the  
30  
31  
32  
33  
34  
35  
36  
37  
38  
39  
40  
41  
42  
43  
44  
45  
46  
47  
48  
49  
50  
51  
52  
53  
54  
55  
56  
57  
58  
59  
60

control doping samples, which showed a clear enhancement in the exciton PL intensity upon introduction of the other cations that do not necessarily dope the NC lattice (Figure 3d). These Li<sup>+</sup> and Ca<sup>2+</sup> doped CdSe samples also showed similar charge/PL correlations as when doping with Ag<sup>+</sup>.

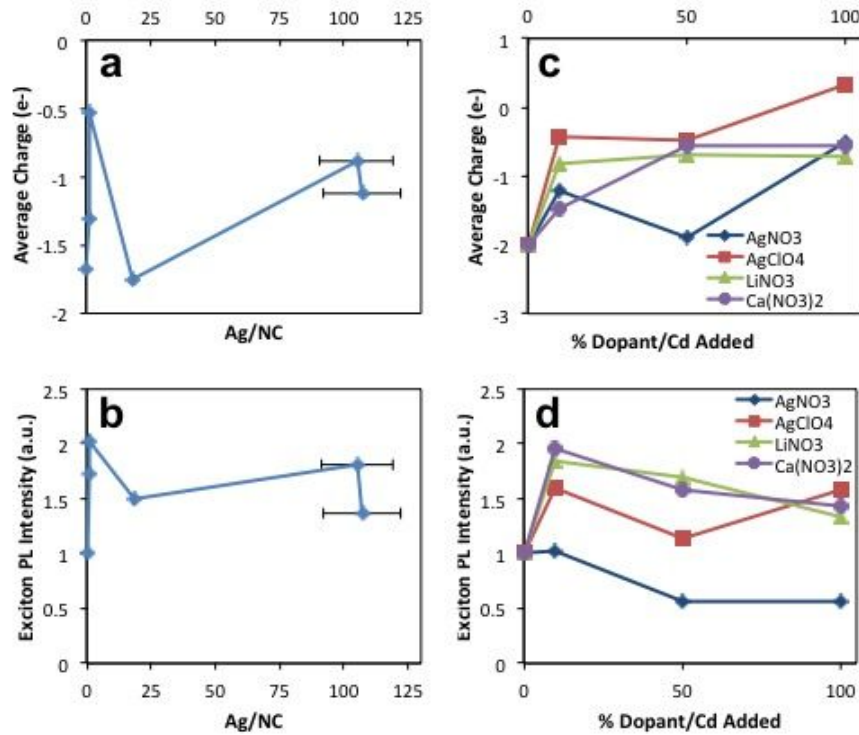


Figure 3. (a,c) Average charges for (a) the trial of Ag<sup>+</sup> doping and (c) the series of control doping trials with AgNO<sub>3</sub>, AgClO<sub>4</sub>, LiNO<sub>3</sub>, and Ca(NO<sub>3</sub>)<sub>2</sub>. (b,d) The maximum exciton PL intensities for (b) a trial of Ag<sup>+</sup> doping and (d) a series of control doping trials.

In total, the EFM and PL data suggest that simply exposing NCs to anions and cations during the cation exchange process, including the Ag<sup>+</sup> ions, is actually causing the PL/charge changes that we and others have observed. Thus, the PL enhancement is not a direct result of dopant type, but rather a result of passivation of the NC surface and/or the creation of an

1  
2  
3 electrostatic field inside the NC, both possibilities suggested by electrochemical measurements  
4 of the  $\xi$ -potential for similar systems.<sup>50</sup>  
5  
6

7 We propose that the changes in exciton PL and the demonstrated correlation between PL  
8 intensity and average NC charge result from the effects of symmetry breaking of the NC due to  
9 the presence of off-center fixed charges. In CdSe NCs, the lowest energy exciton state is  
10 optically dark due to the spin selection rule.<sup>51</sup> Recent theoretical work has showed that charged  
11 defect centers can break the NC symmetry allowing for a brightening of the lowest exciton state  
12 in CdSe NCs.<sup>52</sup> Specifically, depending on the location of the defect centers with respect to the  
13 NC crystal lattice orientation, the resulting breaking of inversion symmetry can lead to up to a  
14 10-fold increase in the radiative rate, with a coinciding increase in the PL quantum yield.<sup>52</sup> This  
15 model was then extended to consider different configurations of charge and compensating  
16 counter-charges to investigate their effects on the radiative lifetime and PL and absorption  
17 spectra.<sup>53</sup>  
18  
19

20 Here we modeled the Ag<sup>+</sup> doped NCs with a set of simplified configurations of positive  
21 charges representing the Ag<sup>+</sup> dopants and negative charges representing counter-ions, as shown  
22 in Figure 4a. Leveraging the recently developed theoretical model for the symmetry-breaking  
23 effect of a charged center on exciton fine structure and level mixing,<sup>41,52,53</sup> we calculated using a  
24 four-band effective mass model that incorporates exchange and axial field effects that a selection  
25 of these structures gave an increased radiative rate over an undoped NC, with the same order of  
26 magnitude as we and others have observed in the brightening of the NC PL (Figure 4b).<sup>25</sup> Note  
27 that in these calculations, correctly accounting for the long-range exchange interaction, as  
28 described in Reference 41, was necessary to properly model the changes in radiative rate.<sup>54</sup> For  
29 the conformations in which we have unbalanced charges, such as those highlighted in green in  
30  
31

1  
2  
3 Figure 4a, we would also expect to see a permanent charge from EFM, whether positive or  
4 negative. Those conformations that demonstrated an increased radiative rate are the same as  
5 those for which we would expect to observe an EFM charge. Conversely, for the configurations  
6 with balanced dopant/counter-ion charges for which we would expect to observe a neutral  
7 particle in EFM, we found little to no increase in the radiative rate.  
8  
9

10  
11 While theory suggests the PL changes due to added charges proceed through modifying  
12 the radiative rate of the NC, an alternative explanation is that the added ions are changing the  
13 non-radiative rate perhaps through interactions with the NC surface. To test this possibility, we  
14 took measurements of the NC PL lifetime and PL efficiency, which allowed for a determination  
15 of changes in radiative and non-radiative decay rates associated with different doping levels.  
16  
17 Raw time-resolved single photon counting PL decay curves and information on the measured  
18 decay rates are given in the SI in Figure S14 and Tables S1 and S2. In short, the trend in the  
19 calculated radiative rates inferred from the time-resolved PL decays and the quantum yield  
20 measurements better matched the changes in the relative oscillator strength for the calculated  
21 configurations (Figure 4b). By contrast, changes in the non-radiative rate extracted from this  
22 analysis were typically much smaller and would result in a much smaller contribution to the  
23 overall PL enhancement if changes in the non-radiative rate were the dominant effect. Thus  
24 overall, the combination of calculations backed by the time-resolved PL measurements provide  
25 evidence that the PL enhancement observed for  $\text{Ag}^+$  doped CdSe is a result of a radiative rate  
26 acceleration caused by symmetry breaking and consequent brightening of the dark exciton state  
27 by the introduced charge.  
28  
29  
30  
31  
32  
33  
34  
35  
36  
37  
38  
39  
40  
41  
42  
43  
44  
45  
46  
47  
48  
49  
50  
51  
52  
53  
54  
55  
56  
57  
58  
59  
60

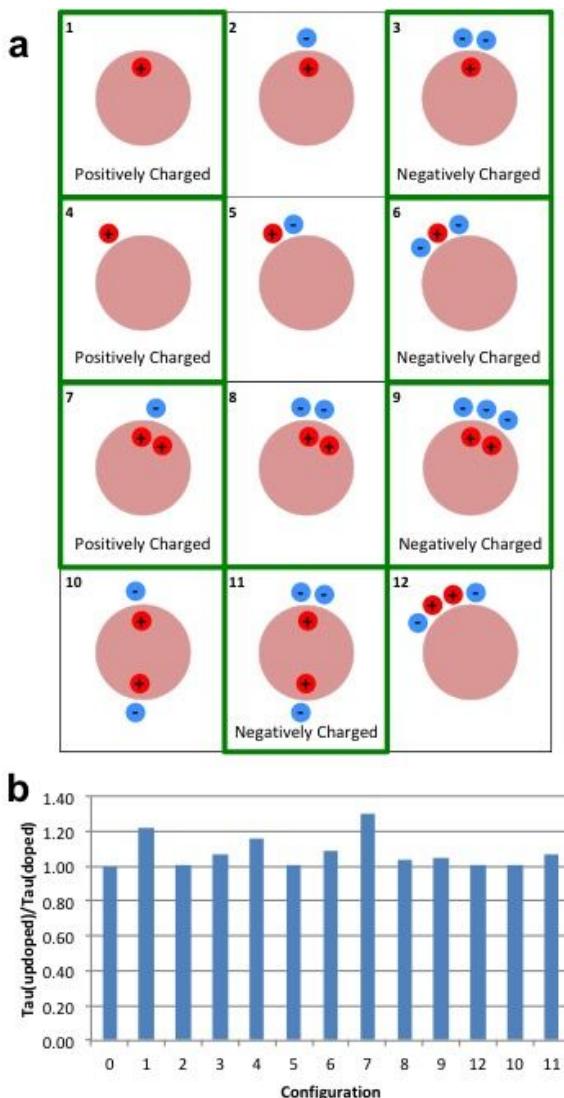


Figure 4. (a) Various configurations of charges within a NC. Positive charges represent  $\text{Ag}^+$  ions and negative charges represent counterions. The configurations highlighted in green are those that presented accelerated radiative rates. (b) Calculated radiative rate acceleration for the various configurations in (a).  $\tau_{\text{u}}$  is the radiative lifetime, which is inversely proportional to the radiative rate.

Note that while we see qualitative agreement between experimental and calculated radiative rates, obtaining exact quantitative agreement would require knowledge of the exact charge placement and distribution with respect to the NC crystal structure. Clearly, this level of knowledge of the doping process down to the single NC level is beyond what is currently possible to experimentally determine. Indeed, the heterogeneity in the cation exchange process

1  
2  
3 creates difficulty in consistently producing identical NC samples due to the natural  
4  
5 irreproducibility of the required post-processing precipitation and washing steps. Coupled with  
6  
7 the inability to precisely characterize and control the chemical nature of NC surfaces down to the  
8 atomic level and the sensitivity in PL to the exact placement of the ions within and on a NC, each  
9 sample doping set is best considered independently. Indeed, there are many combinations of  
10 dopant ions and counterions that can lead to an enhancement in the PL intensity/increase in NC  
11 charge. Thus it is expected that there are a wide variety of possible trends that could be observed  
12 in PL intensity/NC charge with increasing exposure to ions. For illustration, some of these  
13 additional configurations are expressed in the cartoon of Figure S15. Some of these  
14 configurations (those in symmetrical arrangements) can reduce the radiative decay rate while  
15 others (the asymmetrical configurations) can increase the rate, and thus non-monotonic  
16 dependences in PL with respect to amount of Ag added are observed. However, at low doping  
17 concentrations, such as with the introduction of a single charged Coulomb center, an increase of  
18 the radiative decay rate is extracted from the analysis of time-resolved PL data, which is  
19 qualitatively consistent with the calculated effect due to a fixed charged center.

20  
21  
22  
23  
24 While sample heterogeneity makes predicting the changes in charge and PL intensity  
25 across doping levels problematic, there is a clear correlation between NC average charge and PL  
26 intensity. The observed changes are definitely caused by the introduction of the cations, whether  
27 as dopants that enter the NC or as charges that sit near the surface of the NCs. Scanning  
28 transmission electron microscopy-electron energy loss spectroscopy measurements are one  
29 possible route to locate the dopants within the NCs to parse out which configurations of Ag<sup>+</sup>  
30 doped NCs give specific optical and charge results. Combining this physical characterization  
31 with single molecule fluorescence studies will elucidate the effects of doping on the optical  
32  
33  
34  
35  
36  
37  
38  
39  
40  
41  
42  
43  
44  
45  
46  
47  
48  
49  
50  
51  
52  
53  
54  
55  
56  
57  
58  
59  
60

1  
2  
3 properties of the NCs and will help to correlate the dopant quantity and location to the already  
4 established charge/PL intensity connection explained here.  
5  
6

7 In conclusion, cation dopants were introduced to CdSe NCs using a cation exchange  
8 procedure and the resulting photophysical properties were generally comparable to those of  
9 similar systems previously studied. EFM was used to characterize the charge of the doped CdSe  
10 NCs, and an unexpected and remarkable relationship between average charge and ensemble  
11 exciton PL intensity was observed. The NC samples that exhibited an exciton PL intensity  
12 enhancement had greater charge than those that were dimmer. These findings suggest that the  
13 enhancement in PL intensity previously ascribed to the Ag dopants sitting interstitially within the  
14 NC lattice might be better explained by the mere presence of a cation providing a charge that  
15 causes an electric field resulting in increased radiative decay, a proposition supported by both the  
16 experimental results and theoretical work presented here.  
17  
18  
19  
20  
21  
22  
23  
24  
25  
26  
27  
28  
29

30  
31  
32  
33 **Acknowledgements.** This work was supported by the National Science Foundation (NSF)  
34  
35 (CHE-1609365). This work was supported in part by the PARADIM Materials Innovation  
36 Platform (DMR-1539918), and made use of the Cornell Center for Materials Research with  
37 funding from the NSF MRSEC program (DMR-1719875). BHS was supported by NSF GRFP  
38 DGE-1144153. ALE acknowledges support from the U.S. Office of Naval Research through the  
39 U.S. Naval Research Laboratory's core research program. We thank David Norris and Ayash  
40 Sahu for assistance with the doping process and for useful discussions. We would like to thank  
41 Chiara Borrelli and Dustin Trail for help with the ICP-MS measurements and Christine Pratt for  
42 performing the x-ray diffraction measurements. The ICP-MS instrument is partially supported  
43 by a grant from the NSF (EAR-1545637).  
44  
45  
46  
47  
48  
49  
50  
51  
52  
53  
54  
55  
56  
57  
58  
59  
60

1  
2  
3  
4  
5 **Supporting Information Available:**  
6

7 Detailed experimental methods (NC synthesis, doping, and characterization techniques),  
8 electrostatic force microscopy explanation and details, additional sample characterization data,  
9  
10 optical and EFM data for additional  $\text{Ag}^+$  doped CdSe doping sets, optical and EFM data for other  
11  
12 impurity doped samples, and PL lifetime decay curves and lifetime fitting results for  $\text{Ag}^+$  doped  
13  
14 CdSe samples.  
15  
16  
17  
18  
19  
20  
21  
22

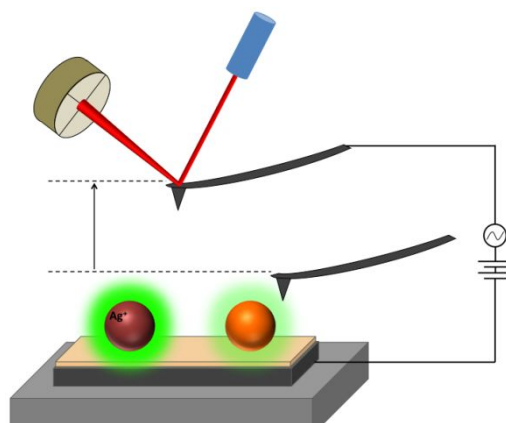
23 **References**  
24

25 1. Alivisatos, A. P. *Science* **1996**, 271, 933-937.  
26  
27 2. Norris, D. J.; Efros, A. L.; Erwin, S. C. *Science* **2008**, 319, 1776-1779.  
28  
29 3. Smith, A. M.; Nie, S. *Acc. Chem. Res.* **2010**, 43, 190-200.  
30  
31 4. Gur, I.; Fromer, N. A.; Geier, M. L.; Alivisatos, A. P. *Science* **2005**, 310, 462-465.  
32  
33 5. Tang, J.; Wang, X.; Brzozowski, L.; Barkhouse, D. A. R.; Debnath, R.; Levina, L.;  
34 Sargent, E. H. *Adv. Mater.* **2010**, 22, 1398-1402.  
35  
36 6. Han, Z.; Qiu, F.; Eisenberg, R.; Holland, P. L.; Krauss, T. D. *Science* **2012**, 338, 1321-  
37 1324.  
38  
39 7. Coe, S.; Woo, W.-K.; Bawendi, M.; Bulovic, V. *Nature* **2002**, 420, 800-803.  
40  
41 8. Eisler, H.-J.; Sundar, V. C.; Bawendi, M. G. *Appl. Phys. Lett.* **2002**, 80, 4614-4616.  
42  
43  
44 9. Rogach, A. L.; Gaponik, N.; Lupton, J. M.; Bertoni, C.; Gallardo, D. E.; Dunn, S.; Li  
45 Pira, N.; Paderi, M.; Repetto, P.; Romanov, S. G.; O'Dwyer, C.; Sotomayor Torres, C. M.;  
46 Eychmüller, A. *Angew. Chem., Int. Ed.* **2008**, 47, 6538-6549.  
47  
48  
49 10. Kim, D. K.; Vemulkar, T. R.; Oh, S.-J.; Koh, W.-k.; Murray, C. B.; Kagan, C. R. *ACS  
50 Nano* **2011**, 5, 3230-3236.  
51  
52  
53 11. Bruchez, M.; Moronne, M.; Gin, P.; Weiss, S.; Alivisatos, A. P. *Science* **1998**, 281, 2013-  
54 2016.  
55  
56 12. Chan, W. C. W.; Nie, S. *Science* **1998**, 281, 2016-2018.  
57  
58  
59

1  
2  
3 13. Michalet, X.; Pinaud, F. F.; Bentolila, L. A.; Tsay, J. M.; Doose, S.; Li, J. J.; Sundaresan,  
4 G.; Wu, A. M.; Gambhir, S. S.; Weiss, S. *Science* **2005**, 307, 538-544.  
5  
6 14. Efros, A. L.; Delehanty, J. B.; Huston, A. L.; Medintz, I. L.; Barbic, M.; Harris, T. D.  
7 *Nature Nanotechnol.* **2018**, 13, 278-288.  
8  
9 15. Murray, C. B.; Norris, D. J.; Bawendi, M. G. *J. Am. Chem. Soc.* **1993**, 115, 8706-8715.  
10  
11 16. Peng, Z. A.; Peng, X. *J. Am. Chem. Soc.* **2001**, 123, 183-184.  
12  
13 17. Son, D. H.; Hughes, S. M.; Yin, Y.; Paul Alivisatos, A. *Science* **2004**, 306, 1009-1012.  
14  
15 18. Beberwyck, B. J.; Surendranath, Y.; Alivisatos, A. P. *J. Phys. Chem. C* **2013**, 117,  
16 19759-19770.  
17  
18 19. Pietryga, J. M.; Werder, D. J.; Williams, D. J.; Casson, J. L.; Schaller, R. D.; Klimov, V.  
19 I.; Hollingsworth, J. A. *J. Am. Chem. Soc.* **2008**, 130, 4879-4885.  
20  
21 20. Manna, L.; Milliron, D. J.; Meisel, A.; Scher, E. C.; Alivisatos, A. P. *Nat. Mater.* **2003**, 2,  
22 382-385.  
23  
24 21. Robinson, R. D.; Sadtler, B.; Demchenko, D. O.; Erdonmez, C. K.; Wang, L.-W.;  
25 Alivisatos, A. P. *Science* **2007**, 317, 355-358.  
26  
27 22. Sadtler, B.; Demchenko, D. O.; Zheng, H.; Hughes, S. M.; Merkle, M. G.; Dahmen, U.;  
28 Wang, L.-W.; Alivisatos, A. P. *J. Am. Chem. Soc.* **2009**, 131, 5285-5293.  
29  
30 23. Bouet, C.; Laufer, D.; Mahler, B.; Nadal, B.; Heuclin, H.; Pedetti, S.; Patriarche, G.;  
31 Dubertret, B. *Chem. Mater.* **2014**, 26, 3002-3008.  
32  
33 24. Mocatta, D.; Cohen, G.; Schattner, J.; Millo, O.; Rabani, E.; Banin, U. *Science* **2011**, 332,  
34 77-81.  
35  
36 25. Sahu, A.; Kang, M. S.; Kompch, A.; Notthoff, C.; Wills, A. W.; Deng, D.; Winterer, M.;  
37 Frisbie, C. D.; Norris, D. J. *Nano Lett.* **2012**, 12, 2587-2594.  
38  
39 26. Pradhan, N.; Goorskey, D.; Thessing, J.; Peng, X. *J. Am. Chem. Soc.* **2005**, 127, 17586-  
40 17587.  
41  
42 27. Deng, Z.; Tong, L.; Flores, M.; Lin, S.; Cheng, J.-X.; Yan, H.; Liu, Y. *J. Am. Chem. Soc.*  
43 **2011**, 133, 5389-5396.  
44  
45 28. Buonsanti, R.; Milliron, D. J. *Chem. Mater.* **2013**, 25, 1305-1317.  
46  
47 29. Zhou, D.; Wang, P.; Roy, C. R.; Barnes, M. D.; Kittilstved, K. R. *J. Phys. Chem. C* **2018**,  
48 122, 18596-18602.  
49  
50 30. Kroupa, D. M.; Hughes, B. K.; Miller, E. M.; Moore, D. T.; Anderson, N. C.;  
51 Chernomordik, B. D.; Nozik, A. J.; Beard, M. C. *J. Am. Chem. Soc.* **2017**, 139, 10382-10394.  
52  
53  
54  
55  
56  
57  
58  
59  
60

1  
2  
3 31. Beulac, R.; Ochsenbein, S. T.; Gamelin, D. R., Colloidal Transition-Metal-Doped  
4 Quantum Dots. In *Nanocrystal Quantum Dots*, Klimov, V. I., Ed. CRC Press: Boca Raton, FL,  
5 2010; p 397.  
6  
7 32. Geyer, S. M.; Allen, P. M.; Chang, L.-Y.; Wong, C. R.; Osedach, T. P.; Zhao, N.;  
8 Bulovic, V.; Bawendi, M. G. *ACS Nano* **2010**, 4, 7373-7378.  
9  
10 33. Gopal, M. B. *Mater. Res. Express* **2015**, 2, 085004.  
11  
12 34. Amit, Y.; Li, Y.; Frenkel, A. I.; Banin, U. *ACS Nano* **2015**, 9, 10790-10800.  
13  
14 35. Whitham, P. J.; Knowles, K. E.; Reid, P. J.; Gamelin, D. R. *Nano Lett.* **2015**, 15, 4045-  
15 4051.  
16  
17 36. Marchioro, A.; Whitham, P. J.; Knowles, K. E.; Kilburn, T. B.; Reid, P. J.; Gamelin, D.  
18 R. *J. Phys. Chem. C* **2016**, 120, 27040-27049.  
19  
20 37. Nelson, H. D.; Hinterding, S. O. M.; Fainblat, R.; Creutz, S. E.; Li, X.; Gamelin, D. R. *J.  
21 Am. Chem. Soc.* **2017**, 139, 6411-6421.  
22  
23 38. Yu, W. W.; Peng, X. *Angew. Chem., Int. Ed.* **2002**, 41, 2368-2371.  
24  
25 39. Bullen, C. R.; Mulvaney, P. *Nano Lett.* **2004**, 4, 2303-2307.  
26  
27 40. Yalcin, S. E.; Labastide, J. A.; Sowle, D. L.; Barnes, M. D. *Nano Lett.* **2011**, 11, 4425-  
28 4430.  
29  
30 41. Krauss, T. D.; Brus, L. E. *Phys. Rev. Lett.* **1999**, 83, 4840-4843.  
31  
32  
33 42. Krishnan, R.; Hahn, M. A.; Yu, Z.; Silcox, J.; Fauchet, P. M.; Krauss, T. D. *Phys. Rev.  
34 Lett.* **2004**, 92, 216803.  
35  
36  
37 43. Cherniavskaya, O.; Chen, L.; Weng, V.; Yuditsky, L.; Brus, L. E. *J. Phys. Chem. B* **2003**,  
38 107, 1525-1531.  
39  
40  
41 44. Yalcin, S. E.; Yang, B.; Labastide, J. A.; Barnes, M. D. *J. Phys. Chem. C* **2012**, 116,  
42 15847-15853.  
43  
44  
45 45. Krauss, T. D.; O'Brien, S.; Brus, L. E. *J. Phys. Chem. B* **2001**, 105, 1725-1733.  
46  
47  
48 46. Geick, R.; Perry, C. H.; Mitra, S. S. *J. Appl. Phys.* **1966**, 37, 1994-1997.  
49  
50 47. Anderson, N. C.; Hendricks, M. P.; Choi, J. J.; Owen, J. S. *J. Am. Chem. Soc.* **2013**, 135,  
51 18536-18548.  
52  
53 48. Kompch, A.; Sahu, A.; Notthoff, C.; Ott, F.; Norris, D. J.; Winterer, M. *J. Phys. Chem. C*  
54 **2015**, 119, 18762-18772.  
55  
56 49. Ott, F. D.; Spiegel, L. L.; Norris, D. J.; Erwin, S. C. *Phys. Rev. Lett.* **2014**, 113, 156803.  
57  
58  
59  
60

1  
2  
3 50. Nag, A.; Chung, D. S.; Dolzhnikov, D. S.; Dimitrijevic, N. M.; Chatopadhyay, S.;  
4 Shibata, T.; Talapin, D. V. *J. Am. Chem. Soc.* **2012**, 134, 13604-13615.  
5  
6 51. Efros, A. L.; Rosen, M.; Kuno, M.; Nirmal, M.; Norris, D. J.; Bawendi, M. *Phys. Rev. B*  
7 **1996**, 54, 4843-4856.  
8  
9 52. Sercel, P. C.; Shabaev, A.; Efros, A. L. *Nano Lett.* **2017**, 17, 4820-4830.  
10  
11 53. Sercel, P. C.; Shabaev, A.; Efros, A. L. *MRS Adv.* **2018**, 3, 711-716.  
12  
13 54. Sercel, P. C.; Efros, A. L. *Nano Lett.* **2018**, 18, 4061-4068.  
14  
15  
16  
17  
18  
19  
20  
21  
22  
23  
24  
25  
26  
27  
28  
29  
30  
31  
32  
33  
34  
35  
36  
37  
38  
39  
40  
41  
42  
43  
44  
45  
46  
47  
48  
49  
50  
51  
52  
53  
54  
55  
56  
57  
58  
59  
60

1  
2  
3  
4  
5  
6  
7  
8  
9  
10  
11  
12  
13  
14  
15  
16  
17  
18  
19  
20  
21  
22  
23  
24  
25  
26  
27  
28  
29  
30  
31  
32  
33  
34  
35  
36  
37  
38  
39  
40  
41  
42  
43  
44  
45  
46  
47  
48  
49  
50  
51  
52  
53  
54  
55  
56  
57  
58  
59  
60  
**For Table of Contents Only**  


ACS Paragon Plus Environment